

## LA-UR-18-25008

Approved for public release; distribution is unlimited.

Title: Thermal Expansion of PBX 9502

Author(s): Menikoff, Ralph

Intended for: Report

Issued: 2018-06-07

---

**Disclaimer:**

Los Alamos National Laboratory, an affirmative action/equal opportunity employer, is operated by the Los Alamos National Security, LLC for the National Nuclear Security Administration of the U.S. Department of Energy under contract DE-AC52-06NA25396. By approving this article, the publisher recognizes that the U.S. Government retains nonexclusive, royalty-free license to publish or reproduce the published form of this contribution, or to allow others to do so, for U.S. Government purposes. Los Alamos National Laboratory requests that the publisher identify this article as work performed under the auspices of the U.S. Department of Energy. Los Alamos National Laboratory strongly supports academic freedom and a researcher's right to publish; as an institution, however, the Laboratory does not endorse the viewpoint of a publication or guarantee its technical correctness.

# THERMAL EXPANSION OF PBX 9502

RALPH MENIKOFF

June 6, 2018

## Abstract

Shock-to-detonation transition experiments for PBX 9502 cover a wide range of temperatures from -196 C to 250 C. The initial density is typically determined from the measured density at room temperature and the coefficient of thermal expansion. Here we combine the fits for the volumetric coefficient of thermal expansion by [Skidmore et al. \[2003\]](#) and for the density by Cady [see [Dallman and Wackerle, 1993](#), fig. 2] to cover the full temperature range of the shock initiation experiments.

# 1 Introduction

The initial density of a PBX is important for determining the detonation wave speed and the CJ state. The density of a PBX is usually measured only at room temperature. At other temperatures the density is inferred from the volumetric coefficient of thermal expansion.

For the insensitive explosive PBX 9502, a fit to the coefficient of thermal expansion has been determined for the temperature interval  $-60 < T < 80$  C by [Skidmore et al. \[2003\]](#). Shock-to-detonation transition (SDT) experiments have been done over a wider range of temperatures; from liquid nitrogen temperature of -196 C [[Hollowell et al., 2014](#)] up to 250 C [[Dallman and Wackerle, 1993](#)]. The purpose of this note is to extend the fit for the coefficient of thermal expansion to cover the full temperature range used in shock initiation experiments.

To extend the fit, we use the high temperature density data of Cady [see [Dallman and Wackerle, 1993](#), fig. 2] and extrapolate [[Skidmore et al., 2003](#)] data to lower temperature. A piecewise cubic fit is determined for  $\rho(T)$  such that the coefficient of thermal expansion is continuous and monotonic.

The accuracy of the coefficient of thermal expansion is limited by several unusual thermal properties of PBX 9502. These are briefly described in the final discussion section.

## 2 Coefficient of thermal expansion

The volumetric coefficient of thermal expansion is defined by

$$\beta(T, P) = V^{-1}(\partial V / \partial T)_P . \quad (1)$$

Hereafter we take  $P = 1$  b and treat thermodynamic variables as functions of only  $T$ . The specific volume as function of temperature is given by

$$V(T) = V_{ref} + \int_{T_{ref}}^T dT V \cdot \beta(T) . \quad (2)$$

It is more convenient to use the secant coefficient of thermal expansion which is defined as

$$CTE(T) = \frac{V(T)/V_{ref} - 1}{T - T_{ref}} . \quad (3)$$

Following [Skidmore et al. \[2003\]](#), for the reference state of PBX 9502 we take  $T_{ref} = 21$  C and  $\rho_{ref} = 1.889$  g/cc. Then the specific volume can be expressed as

$$V(T) = [1 + CTE(T) \cdot (T - T_{ref})] V_{ref} . \quad (4)$$

Alternatively, the density is given by

$$\rho(T) = \frac{\rho_{ref}}{1 + CTE(T) \cdot (T - T_{ref})} , \quad (5)$$

and to leading order in  $T - T_{ref}$  as

$$\rho(T) \approx [1 - CTE(T) \cdot (T - T_{ref})] \rho_{ref} . \quad (6)$$

Thus, by using the secant coefficient an integral is not needed to obtain the density.

### 3 PBX 9502 thermal expansion

A piecewise fit is used to define the density as a function of temperature at 1 bar.

1. Cubic fits over 3 intervals that span the intermediate temperature domain  $-40 < T < 40$  C:  
 $-40 < T < -20$  C,  $-20 < T < 21$  C,  $21 < T < 40$  C  
 The cubic polynomials are determined by matching the values of  $\rho$  and  $d\rho/dT$  at the end points of the intervals to the values of the fit from [Skidmore et al. \[2003, Eq. 7 and fig. 9\]](#) for the coefficient of linear expansion, which is 1/3 volumetric coefficient.
2. Low temperature extrapolation to the interval  $-196 < T < -40$  C.  
 Quadratic fit that matches  $\rho$  and its first 2 derivatives at  $T = -40$  C to the values of the cubic fit in the interval  $-40 < T < -20$  C.
3. High temperature extrapolation to the interval  $40 < T < 252$  C.  
 Cubic fit that matches  $\rho$  and its first 2 derivatives at  $T = 40$  C to values of the cubic in the interval  $21 < T < 40$  C. The third derivative is determined match  $\rho(252\text{ C}) = 1.70\text{ g/cc}$  from Cady [see [Dallman and Wackerle, 1993, fig. 2\]](#).

By construction, at the endpoint of each interval,  $CTE$  and its first derivative are continuous. Hence  $\beta$  is also continuous. Also by construction, at the end points of the extrapolated intervals,  $T = -40$  and  $T = 40$  C, the derivative of  $\beta$  is continuous.

The internal end points of the intermediate intervals,  $T = -20$  and  $T = 21$  C, have been chosen such that the derivative of  $\beta$  has only a small discontinuity, and to preserve the value of  $\rho_{ref}$ . Hence, Eq. (3) can be used to define the secant coefficient of thermal expansion, which only differs slightly from the fit of [Skidmore et al. \[2003, Eq. 7 and fig. 9\]](#). The end points of the intermediate interval  $T = -40$  and  $T = 40$  C have been chosen such that  $\beta$  is monotonic.

The numerical fits for each interval are as follows:

$$\underline{-196 < T < -40 \text{ C}}$$

$$\begin{aligned} \rho(T) &= 1.90588 - 2.54307e-04 \Delta T - 1.75145e-07 \Delta T^2, \\ \text{where } \Delta T &= T + 40. \end{aligned} \quad (7a)$$

$$\underline{-40 < T < -20 \text{ C}}$$

$$\begin{aligned} \rho(T) &= 1.90588 - 2.54307e-04 \Delta T - 1.75145e-07 \Delta T^2 - 2.88904e-10 \Delta T^3, \\ \text{where } \Delta T &= T + 40. \end{aligned} \quad (7b)$$

$$\underline{-20 < T < 21 \text{ C}}$$

$$\begin{aligned} \rho(T) &= 1.90072 - 2.61659e-04 \Delta T - 6.48483e-08 \Delta T^2 - 1.28071e-08 \Delta T^3, \\ \text{where } \Delta T &= T + 20. \end{aligned} \quad (7c)$$

$$\underline{21 < T < 40 \text{ C}}$$

$$\begin{aligned} \rho(T) &= 1.88900 - 3.31563e-04 \Delta T - 1.77388e-06 \Delta T^2 - 2.43455e-08 \Delta T^3, \\ \text{where } \Delta T &= T - 21. \end{aligned} \quad (7d)$$

$$\underline{40 < T < 252}$$

$$\begin{aligned} \rho(T) &= 1.88189 - 4.25337e-04 \Delta T - 3.19374e-06 \Delta T^2 + 5.43839e-09 \Delta T^3, \\ \text{where } \Delta T &= T - 40. \end{aligned} \quad (7e)$$

The secant coefficient of thermal expansion is then given by

$$CTE(T) = \frac{\rho_{ref}/\rho(T) - 1}{T - T_{ref}} \quad (8a)$$

for  $T \neq T_{ref}$  and to leading order around  $T_{ref}$  by

$$\begin{aligned} CTE(T) &= -\rho_{ref}^{-1}(\mathrm{d}\rho/\mathrm{d}T)(T_{ref}) + \left( 2 [\rho_{ref}^{-1}(\mathrm{d}\rho/\mathrm{d}T)(T_{ref})]^2 - \rho_{ref}^{-1}(\mathrm{d}^2\rho/\mathrm{d}T^2)(T_{ref}) \right) (T - T_{ref}) \\ &= \beta(T_{ref}) + [2\beta^2(T_{ref}) - \rho_{ref}^{-1}(\mathrm{d}^2\rho/\mathrm{d}T^2)(T_{ref})] (T - T_{ref}). \end{aligned} \quad (8b)$$

Plots of the fits for the density along with the coefficient of thermal expansion and secant coefficient are shown in fig. 1. We note that the slope of  $\beta$  changes rapidly around  $T_{ref}$ , that is, room temperature. Since the secant coefficient CTE is an average over  $\beta$ , which follows from Eq. (2) and Eq. (3), the change in its slope is less pronounced. The change in slope is due to the glass transition in the Kel-F binder ( $T_g \approx 28 \text{ C}$ ), which has a significant effect on its coefficient of thermal expansion [see Thompson et al., 2018, fig. 7].

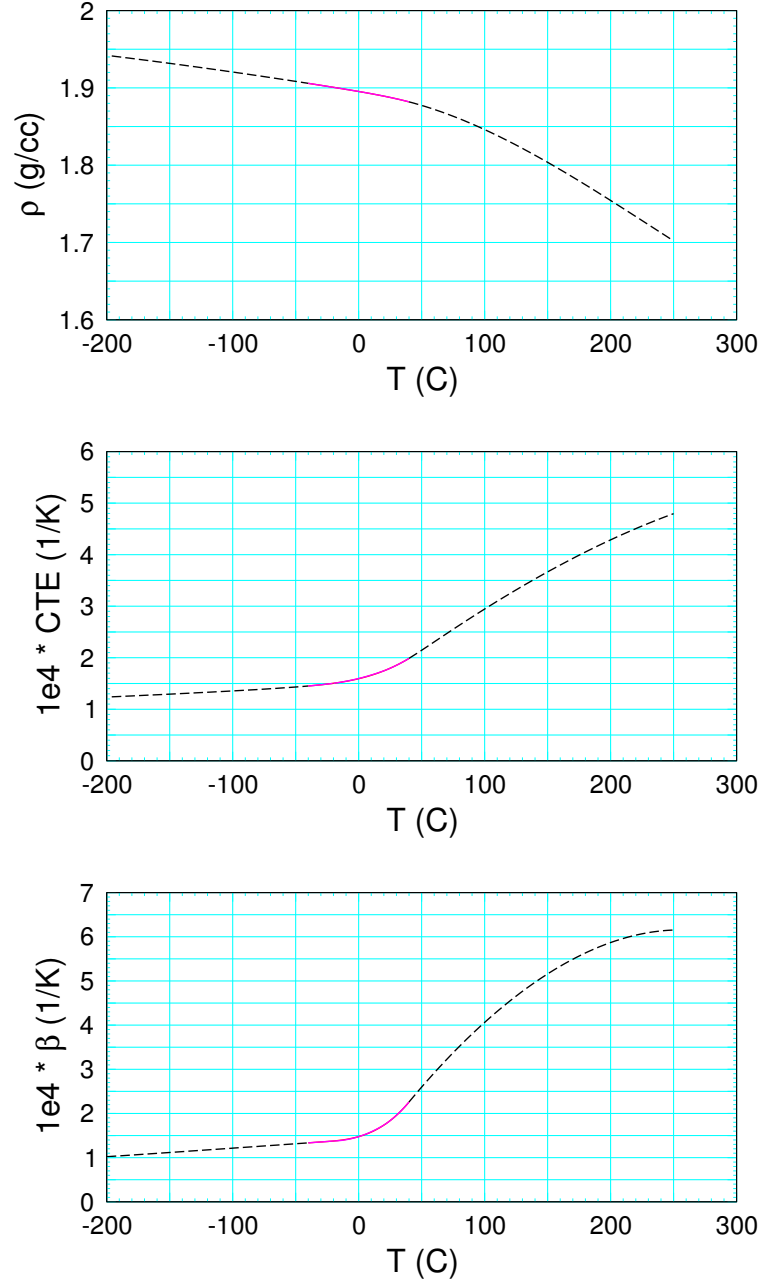


Figure 1: Density, CTE,  $\beta$ . Dashed lines are extrapolation of CTE fit of [Skidmore et al., 2003].

## 4 Discussion

A fit of  $\rho(T)$  at  $P = 1$  b has been developed for PBX 9502 that covers the full temperature range,  $-196 < T < 252$  C or equivalently  $77 < T < 523$  K, of shock initiation experiments. The fit for  $\rho(T)$  is constructed to be consistent with the thermal expansion data of [Skidmore et al. \[2003\]](#) and Cady [see [Dallman and Wackerle, 1993](#), fig. 2]. From the density fit, the secant coefficient of thermal expansion can readily be calculated.

PBX 9502 is composed of 95 wt % dry-aminated TATB and 5 % Kel-F 800 binder. It also has a couple of per cent porosity, some of which are holes or pits in the surface of the TATB grains. Changes of porosity with temperature contribute to the thermal expansion of PBX 9502.

PBX 9502 has several unusual thermal properties that leads to a scatter in the thermal expansion data and limits the accuracy of any fit for the coefficient of thermal expansion. TATB has a graphitic crystal structure and its thermal expansion is very anisotropic. As pointed out by [Skidmore et al. \[2003\]](#) and others, thermal expansion of PBX 9502 is also anisotropic due to partial alignment of TATB grains in the way the PBX is manufactured; the normal to the graphitic-like planes tend to align with pressure gradient in the pressing process.

In addition, there is an increase in volume (or decrease in density) with thermal cycling known as ratchet growth; see [[Thompson et al., 2018](#), fig. 1] and references therein. Ratchet growth results in irreversible changes in the porosity distribution [[Thompson et al., 2010](#)] and the effects are cumulative with the number of cycles. The decreased density is important since it results in an increase in the shock sensitivity [[Gustavsen et al., 2010](#)].

The TATB exotherm shows no reaction below 310 C [see [Gibbs and Popolato, 1980](#), p. 158, fig. 2]. However, thermal expansion experiments have observed PBX 9502 weight loss at 250 C [see [Dallman and Wackerle, 1993](#), fig. 1]. [Maienschein and Gracia \[2002\]](#) attribute the mass loss to sublimation of TATB. This is surprising as the TATB vapor pressure is very low; extrapolating data in [[Östmark et al., 2012](#), fig. 7 and table 2] the vapor pressure is  $1.3\text{e-}5$  b at 252 C.

Kel-F is a co-polymer. Depending on its crystallinity, it undergoes a glass transition at about 28 C and melts at about 80 C; see [[Cady and Caley, 1977](#)]. It does not decompose until 300 C. We note that the high temperature SDT experiments are under the decomposition temperature but well above the melt temperature. In this regime the Kel-F is a viscous liquid.

LX 17 is a similar high explosive to PBX 9502. It is composed of 92.5 wt % wet-aminated TATB and 7.5 % Kel-F 800 binder. High temperature thermal expansion experiments have also been performed on LX 17. Above 300 K [Maienschein and Gracia \[2002\]](#), fig. 5 and Eq. 7] found that CTE is linear in temperature. The fit of PBX 9502 in fig. 1 shows that above 50 C (323 K) CTE is approximately linear but the slope is about 50 % larger. This could be due to different

pressing methods in the manufacture of the samples. Alternatively, wet- vs dry-aminated TATB have different crystal morphology and also results in differences in impurities. Also, [Maienschein and Gracia \[2002, fig. 3\]](#) have shown that the thermal expansion of LX 17 is affected by pressing temperature.

The conclusion that can be drawn from this discussion is that the nature of the heterogeneities within a piece of PBX 9502 matter. The fit for the coefficient of thermal expansion derived here is applicable to pieces of PBX 9502 that were manufactured in a similar manner to the samples used for the data on which the fits are based.

## References

- W. E. Cady and L. E. Caley. Properties of Kel F-800 polymer. Technical report, Lawrence Livermore National Lab., July 1977. UCRL-52301, <https://doi.org/10.2172/5305005>. 6
- J. C. Dallman and J. Wackerle. Temperature-dependent shock initiation of TATB-based high explosive. In *Tenth Symposium (International) on Detonation*, pages 130–138, 1993. 1, 2, 3, 6
- T. R. Gibbs and A. Popolato, editors. *LASL Explosive Property Data*. Univ. of Calif. Press, 1980. URL <http://lib-www.lanl.gov/ladcdmp/epro.pdf>. 6
- R. L. Gustavsen, D. G. Thompson, B. W. Olinger, R. DeLuca, B. D. Bartram, T. H. Pierce, and N. J. Sanchez. Shock initiation experiments on ratchet grown PBX 9502. In *Fourteenth Symposium (International) on Detonation*, pages 655–663, 2010. 6
- B. C. Hollowell, R. L. Gustavsen, and D. M. Dattelbaum. Shock initiation of TATB-based explosive PBX 9502 cooled to 77 Kelvin. *J. Phys. Conf. Series*, 500, 2014. URL <http://dx.doi.org/10.1088/1742-6596/500/18/182014>. 2
- J. L. Maienschein and F. Gracia. Thermal expansion of TATB-based explosives from 300 to 566 K. *Thermochimica Acta*, 384:61–83, 2002. URL [https://doi.org/10.1016/S0040-6031\(01\)00778-X](https://doi.org/10.1016/S0040-6031(01)00778-X). 6, 7
- H. Östmark, S. Wallin, and H. G. Ang. Vapor pressure of explosives: A critical review. *Propellants Explosives Pyrotechnics*, 37:12–23, 2012. URL <https://doi.org/10.1002/prep.201100083>. 6

- C. B. Skidmore, T. A. Butler, and C. W. Sandoval. The elusive coefficient of thermal expansion in PBX 9502. Technical report, Los Alamos National Lab., January 2003. LA-14003, <https://www.osti.gov/scitech/servlets/purl/809945>. 1, 2, 3, 5, 6
- D. G. Thompson, G. W. Brown, B. Olinger, J. T. Mang, B. Patterson, R. DeLuca, and S. Hagelberg. The effects of TATB ratchet growth on PBX 9502. *Propellants Explosives Pyrotechnics*, 35:507–513, 2010. URL <http://dx.doi.org/10.1002/prop.200900067>. 6
- D. G. Thompson, C. S. Woznick, and R. DeLuca. The volumetric coefficient of thermal expansion of PBX 9502. Technical report, Los Alamos National Lab., March 2018. LA-UR-18-22138, <https://doi.org/10.2172/1425787>. 4, 6